ACS APPLIED MATERIALS & INTERFACES

RESEARCH ARTICLE

www.acsami.org

Novel Bolaamphiphilic Pyrimidinophane As Building Block for Design of Nanosized Supramolecular Systems with Concentration-Dependent Structural Behavior

Mikhail A. Voronin,[†] Dinar R. Gabdrakhmanov,[†,‡] Vyacheslav E. Semenov,[†] Farida G. Valeeva,[†] Anatoly S. Mikhailov,[†] Irek R. Nizameev,[†] Marsil K. Kadirov,[†,‡] Lucia Ya. Zakharova,*[,†,‡] Vladimir S. Reznik,[†] and Alexander I. Konovalov[†]

[†]A. E. Arbuzov Institute of Organic and Physical Chemistry of the Russian Academy of Sciences, 8, ul.Akad. Arbuzov, Kazan, 420088, Russia

[‡]Kazan State Technological University, 68, ul. K. Marx, Kazan, 420015, Russia

Supporting Information

ABSTRACT: A new macrocyclic bolaamphiphile with thiocytosine fragments in the molecule (B1) has been synthesized and advanced as perspective platform for the design of soft supramolecular systems. Strong concentration-dependent structural behavior is observed in the water-DMF (20% vol) solution of B1 as revealed by methods of tensiometry, conductometry, dynamic light scattering, and atomic force microscopy. Two breakpoints are observed in the surface tension isotherms. The first one, around 0.002 M, is identified as a critical micelle concentration (cmc), whereas the second critical concentration of 0.01 M is a turning point between the two models of the association involved. Large aggregates of ca. 200 nm are mostly formed beyond the cmc, whereas small micelle-like aggregates exist above 0.01 M. The growth of aggregates between these critical points occurs, resulting in a gel-like behavior. An unusual decrease in the solution pH with concentration takes place, which is assumed to originate from the steric hindrance around the B1 head groups. Because of controllable structural behavior, B1 is assumed to be a candidate for the development of biomimetic catalysts, nanocontainers, drug and gene carriers, etc.

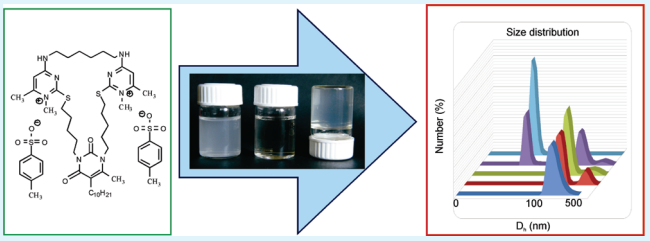

KEYWORDS: bolaamphiphile, pyrimidinophane, self-organization, gel, concentration-dependent

INTRODUCTION

Self-assembling systems play a key role in the development of advanced technologies in medicine, biology, ecology, cosmetics, coating, oil industry, etc.[1−3] Their current relevance is based on the capacity of amphiphilic compounds including those of a cyclophane nature to associate spontaneously and to interact with various practically important substrates via the "guest-host" mechanism. The "bottom-up" strategy underlying the supramolecular approach makes it possible to control the properties of the ensembles formed through the directed variation of the structure of the amphiphilic building blocks. Therefore, the design of new amphiphilic compounds is a challenging task. Meanwhile, researchers are nowadays faced with a number of criteria whereby amphiphiles are assumed to be biocompatible, ecological, associating at low concentrations, stimuli-responsive, and so on. In accordance with these challenges, several lines of investigation are now formed, including those concerning gemini and cleavable surfactants, amphiphiles with natural fragments in the molecules, i.e., amino acids, nitrogen bases, steroids, etc.[4−10] Another important direction is the design of responsive material. Supramolecular systems are formed and function due to non-covalent interactions, which allow them to easily rearrange and adjust to various conditions. Thus, the development of soft materials, including the temperature, pH or concentration responsive systems became accessible.[11−17] The present study focuses on these problems.

The following aspects are assumed to be considered. (i) Synthesis of a new bolaamphiphile with a thiocytosine fragment in the molecule (**B1**) (Scheme 1). Our idea is to combine lipid fragments with nucleotide bases, in particular cytosine and uracil derivatives in a macrocyclic framework. In our opinion, consolidation of nucleotide base ability to aromatic π-stacking interactions, hydrophobic effect, van der Waals, and hydrogen bonds[18−21] on the one hand and the amphiphilic nature and rigid macrocyclic structure on the other is a promising approach. Hybrid molecules and macromolecules combining nucleic acids and lipids have therefore attracted significant attention, as for example in the design of artificial molecular devices, and novel therapeutic strategies.[22]

Received: October 16, 2010
Accepted: January 2, 2011
Published: January 24, 2011

dx.doi.org/10.1021/am101000j | *ACS Appl. Mater. Interfaces* 2011, 3, 402–409

Scheme 1. Chemical Structure of B1

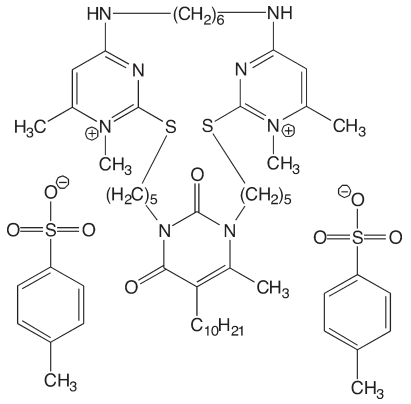

Amphiphilic nucleoside and nucleotide derivatives are well-known.[22] In our group, acyclic and macrocyclic non-glycosidic amphiphilic uracils were developed and some features of these compounds were described.[23−25] Herein the goal is the introduction of cytosine derivatives in the macrocyclic framework, in particular 6-methylthiocytosine (6-methyl-2-thio-4-aminopyrimidine) fragments linked to each other and the uracil unit with polymethylene bridges. To the best of our knowledge, amphiphilic cytosine derivatives have not been described so far.

(ii) The elucidation of self-organization of **B1**. Synthesis and applications of geminis and bolas are the perspective directions of modern supramolecular chemistry.[26−38] Bolaamphiphiles or bolaform surfactants or bolas are molecules that have a hydrophilic group at both ends of the hydrophobic chain.[26−30] Gemini surfactants consist of two hydrophobic chains and two hydrophilic headgroups linked by a spacer that can be both long or short and flexible or rigid.[31−38] Because of their structural features, bolas and geminis demonstrate a marked ability for self-organization at the interface or in bulk solutions.[26−38] Spontaneous curvature of the aggregates formed in aqueous solutions is strongly determined by the geometry of molecules, the nature of spacer, hydrophilic-lipophilic balance, etc. Macrocyclic bolas, in particular pyrimidinophanes, provide an additional possibility for the design of supramolecular architectures because of the involvement of a wider spectrum of intermolecular bonds, i.e., stacking effects, inclusion interactions with the partition of the cavity, hydrogen bonds, etc. As was previously reported, diverse packing modes occur in the systems based on cyclophanes, including pyrimidinophanes.[23,39] Two models of association are shown to be involved in these systems.[40] They are a closed model, which is typical for surfactants and results in the formation of small micelle-like aggregates, and an open model occurring for biorelevant amphiphiles including drugs. This results in the formation of large aggregates exhibiting a layer or a stacklike packing mode.

(iii) One of the problems of interest for us is the structural rearrangements of self-assembling systems, including percolation in reverse microemulsion, a "sphere-rod" and "isotropic phase-mesophase" transitions, etc.[41,42] The design of liquid crystalline and gel systems is of great importance from the viewpoint of optic electronics, cosmetics, oil industry, etc. Therefore, this work focused on the structural behavior of aggregates under the varied conditions.

EXPERIMENTAL SECTION

The ^{1}H NMR spectra were recorded on Avance IITM-400 spectrometer with Me_4Si as the internal standard. MALDI-TOF mass spectra were obtained on a Bruker ULTRAFLEX mass spectrometer in p-nitroaniline matrix. Microanalyses of C, H, and N were performed with a CHN-3 analyser. The melting point was measured on a Boetius hot-stage apparatus. Thin layer chromatography was performed on Silufol-254 plates; visualization was carried out with UV light. For column chromatography, silica gel of 60 mesh from Fluka was used. All solvents were dried according to standard protocols.

Pyrimidinophane (1). A mixture of disodium salt of *N,N′*-(hexane-1,6-diyl)-bis(4-amino-6-methylpyrimidine-2-thione) **2**[43] (4.10 g, 10 mmol) and 1,3-bis(bromopentyl)-5-n-decyl-6-methyluracil **3**[44] (5.0 g, 10 mmol) was stirred in DMF (400 mL) at room temperature for 30 h. The solvent was evaporated in vacuo. The residue was subjected to column chromatography using successive elution with hexane, diethyl ether, and 1:1 ethyl acetate-diethyl ether mixture. From the ethyl acetate-diethyl ether mixture fractions macrocycle **1** (0.77 g, 10%) was obtained; white crystals; mp 115−117°C. Found: C, 64.27; H, 8.60; N, 14.63; S, 8.29. Calcd for $C_{41}H_{66}N_8S_2O_2$: C, 64.19; H, 8.67; N, 14.61; S, 8.36%. δH (400 MHz, $CDCl_3$, [ppm]): 0.88 (t, 3H, CH_3, J = 7.2 Hz), 1.26 (m, 12H, $6CH_2$), 1.41 (m, 4H, $2CH_2$), 1.49 (m, 4H, $2CH_2$), 1.61−1.79 (m, 16H, $8CH_2$), 2.23, 2.24, 2.25 (all s, 3H each, $C^6_{ur}CH_3$, $2C^6_{pyr}CH_3$), 2.41 (t, 2H, $C^5_{ur}CH_2$, J = 6.8 Hz), 3.01−3.09 (m, 4H, $2SCH_2$), 3.30 (m, 4H, $2NHCH_2$), 3.83 (m, 2H, $N^1_{ur}CH_2$), 3.94 (m, 2H, $N^3_{ur}CH_2$), 5.15 (br. s, 2H, 2NH), 5.81, 5.83 (both s, 1H each, $2C^5_{pyr}H$). MALDI−TOF mass spectrum: calcd for $C_{41}H_{67}N_8S_2O_2$ $[M + H]^+$: 767.5. Found: 767.8.

Bolaamphiphilic Pyrimidinophane B1. A mixture of pyrimidinophane **1** (0.75 g, 1 mmol) and 4.5 g of methyl *p*-toluenesulfonate was stirred for 7 h at 100°C. The mixture was cooled to room temperature, 100 mL of diethyl ether was added, and the liquid phase was separated from the precipitate by decanting. This procedure was repeated 5 times, and the oily product was dried under reduced pressure. Found: C, 60.00; H, 7.52; N, 9.80; S, 11.33. Calcd for $C_{57}H_{86}N_8S_4O_8$: C, 60.07; H, 7.61; N, 9.83; S, 11.26%. δH (400 MHz, $CDCl_3$, [ppm]): 0.88 (t, H, CH_3, J = 6.7), 1.26−1.78 (m, 36H, $18CH_2$), 2.21 (s, 3H, $C^6_{ur}CH_3$), 2.30 (br. s, 14H, $C^5_{ur}CH_2$, $2C_{Ar}CH_3$, $2C^6_{pyr}CH_3$), 3.13−3.60 (m, 14H, $2SCH_2$, $2NHCH_2$, $2N^+CH_3$), 3.78 (m, 2H, $N^1_{ur}CH_2$), 3.88 (m, 2H, $N^3_{ur}CH_2$), 6.73 (br. s, 2H, $2C^5_{pyr}H$), 7.11, 7.68 (both br.s, 4H each, $8C_{Ar}H$), 8.94 (br. s, 2H, 2NH). MALDI−TOF mass spectrum: calcd for $C_{50}H_{79}N_8S_3O_5$ $[M\text{-}OTs]^+$, $[M\text{-}2OTs]^+$, $[M\text{-}2OTs\text{-}CH_3]^+$, $[M\text{-}2OTs\text{-}2CH_3]^+$: 967.5, 796.5, 781.5, 766.5. Found: 967.7, 796.7, 781.7, 766.7.

Dynamic light scattering (DLS) measurements were performed by means of the PhotoCor Complex and Malvern Instrument Zetasizer Nano. The measured autocorrelation functions were analyzed by Malvern DTS software, the Dynals program and the second-order cumulant expansion methods. The effective hydrodynamic radius (R_h) was calculated according to the Einstein-Stokes relation: $D_S = k_BT/6\pi\eta R_h$, in which D_S is the diffusion coefficient, k_B is the Boltzmann constant, T is the absolute temperature, and η is the viscosity. The diffusion coefficient was measured at least three times for each sample. The average error in these experiments was approximately 4%. The solutions were filtered with Millipore filters, to remove dust particles from the scattering volume. The experimental details are described elsewhere.[45] Zeta potential Nano-ZS (MALVERN) with laser Doppler velocimetry and phase analysis light scattering was used for zeta potential measurement. The temperature of the scattering cell was controlled at 25 °C; the data were analyzed with the software supplied for the instrument. The viscosity was measured by using Vibro Viscosimeter SV-10 (Japan) as a unit of Zetasizer Nano complex.

An atomic force microscope (MultiMode V, USA) was used to investigate the size and morphology of the particles. The 250−350 kHz cantilevers (Veeco, USA) with silicone tips were used in all measurements. Tip curvature radius is of 10−13 nm. The microscopic images were obtained by means of 8279JV scanner with a 256 × 256 resolution.

Scheme 2. Reagents and Conditions: (i) DMF, rt, 30h; (ii) CH_3OTs, 100°C, 7 h

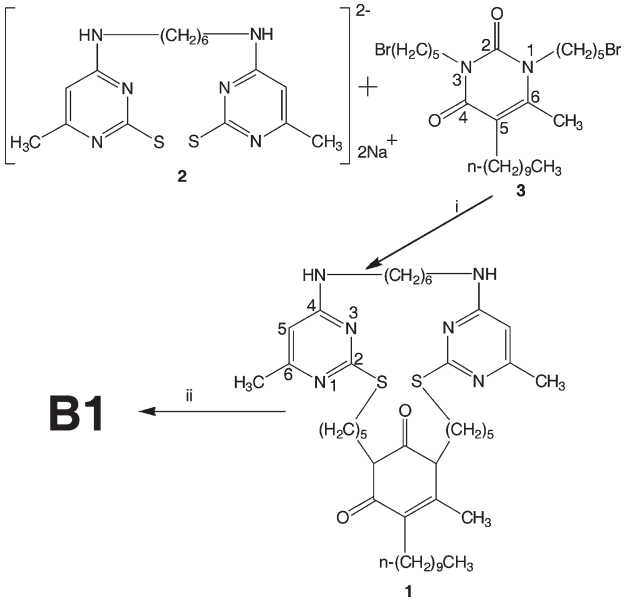

The scanning rate was 1 Hz. The antivibrational system (SG0508) was used to eliminate external distortions. The aqueous dispersions of the sample were placed on the mica surface with the roughness no more than 1−5 nm. The AFM imaging was performed after solvent evaporation.

Conductivity measurements were performed using an inoLab Cond Level 1 instrument. Surface tension measurements were performed using the du Nouy ring detachment method. The experimental details are described elsewhere.[46] Solution pH were monitored with the help of pH-meter HI 9025 ("Hanna Instruments", Germany) using glass membrane electrode HI 1330.

RESULTS AND DISCUSSION

Synthesis. Bolaamphiphilic pyrimidinophane **B1** has been synthesized by the reaction of pyrimidinophane **1** with methyl p-toluenesulfonate (tosylate). The reaction was carried out in the ester and it was used as a reagent and as a solvent. The unambiguous assignment of the structure of amphiphilic macrocyclic bissulfonate **B1** with onium centers on N^1 in the 6-methylthiocytosine fragments is realized on the basis of elemental analysis and NMR spectra, especially $^1H-^{13}C$ HMBC and $^1H-^{15}N$ HMBC correlation experiments in the way as it was described for model systems.[47] The details of this assignment for the macrocycle and the related compounds will be published elsewhere. The initial macrocycle **1** was prepared by the established procedure,[48] in particular, the reaction of disodium salt **2** with dibromide **3** (Scheme 2).

Visual Observations. Pyrimidinophane **B1** showed restricted solubility in water, and therefore the aggregation behavior in the water-DMF (20% vol) has been studied. A series of samples are prepared by a stepwise dilution of the initial stock solution of 0.03 M. The concentration-dependent changes visualized in the course of the procedure are as follows. The transition from transparent solutions at high dilution (≤0.0001 M) to opalescent samples with turbidity occurs within the concentration range limited by ca.0.003 M, whereupon the solutions become transparent again. At the concentration of 0.009 M a sharp decrease in the fluidity is observed, and the gel-like system is formed upon aging for 24 h (Figure 1). The singularity of this sample and its tendency toward the solidification are in line with the viscosity data (Figure 2). All samples with concentrations exceeding 0.009 M are quite transparent and fluid, however they manifest reversible gel-like behavior when the temperature decreases ≤ 20 °C. To elucidate these transitions, we studied solution behavior of **B1** by methods of tensiometry, potentiometry, conductometry, dynamic light scattering, and atomic force microscopy (AFM).

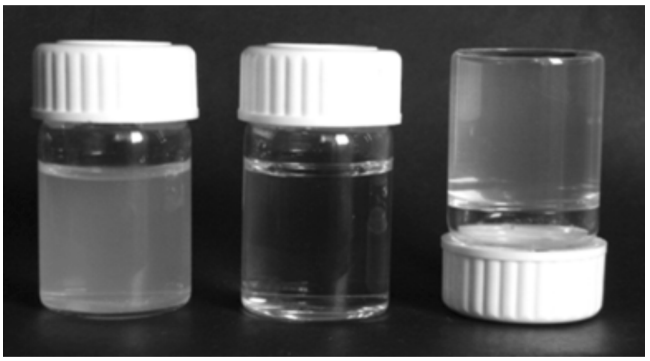

Figure 1. Samples of the water-DMF (20% vol) **B1** solutions; left to right (concentration): 0.0008, 0.005, 0.009 M.

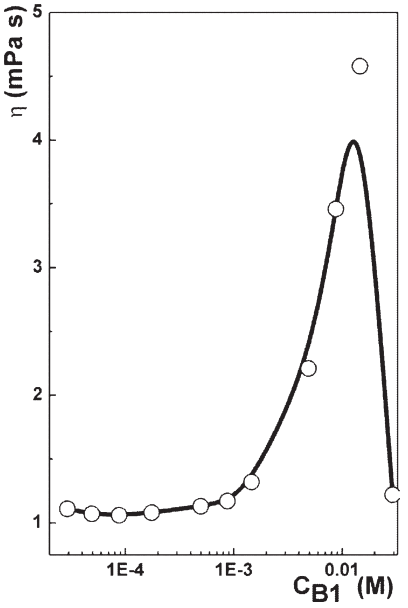

Figure 2. Dynamic viscosity versus concentration dependence for the water-DMF (20% vol) **B1** solution; 25 °C.

Extraction of Critical Micelle Concentration (cmc) by Methods of Tensiometry and Conductometry. These two methods are routine techniques for the examination of the aggregation in the ionic surfactant based systems, which are urged to answer questions, (i) if the aggregation does occur; (ii) whether association is cooperative; (iii) if so, what is the cmc value. As can be seen from Figure 3, a sharp decrease in the surface tension is observed with the **B1** concentration, i.e. the typical surfactant behavior occurs. The plot exhibits a breakpoint at the concentration of 0.0017 M.

Jumplike changes in surface tension occurring at this concentration indicate the cooperative character of association and make it possible to identify it as a cmc value. Meanwhile, unlike

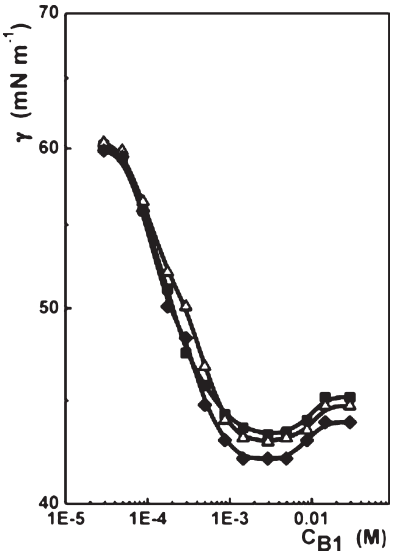

Figure 3. Surface tension isotherm of the water-DMF (20% vol) **B1** solution, fresh solution (■), after 3 days (Δ), after 5 days (♦); 25 °C.

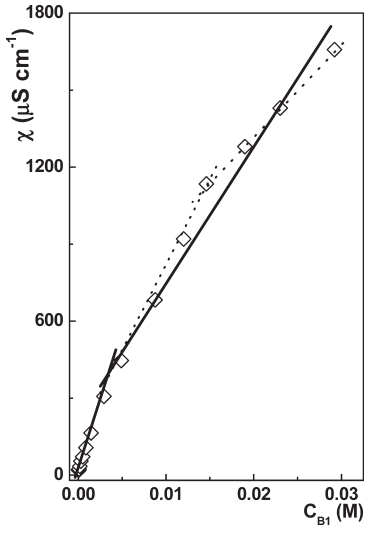

Figure 4. Specific conductivity versus concentration dependence for the water-DMF (20% vol) **B1** solution; 25 °C.

typical surfactant solutions, the plateau in the surface tension isotherm gives place to raising the γ value within the concentration range between cmc and ca. 0.01 M. The presence of the second critical point around 0.01 M may reflect structural rearrangement in the system; however, this assumption requires further confirmation with using alternative methods. It is worthy of attention that no remarkable changes occur in the γ vs concentration dependence in the process of time (Figure 3), which stands for the reliability of the data.

Figure 4 shows conductometry versus concentration dependence, which demonstrate a breakpoint in the concentration range close to the tensiometry cmc value. The experimental points above the cmc are acceptably described by single straight line (coefficient of correlation $R = 0.98$) (see Table 1S in the Supporting Information), whereas the better linear fitting may be reached, when the second breakpoint beyond 0.01 M is nominated (the dot lines in the plot). This case is consistent with the two breakpoints in the tensiometry dependence. More detailed information on linear regression parameters are given in Figure 1S and Table 1S (see the Supporting Information). The validity of the second breakpoint is supported by the fact that the value of first break point changes from 0.0051 to 0.0026 M, when second break point is nominated. The value of 0.0026 M is more consistent with the tensiometry cmc of 0.0017 M.

Table 1. Cmc Values, Surface Excess, Γ_{max}, Surface Area Per Headgroup, A_{min} for B1 Solution and for Reference Compounds: Decylpyridinium Chloride (DPC),[49] a Gemini Analogue 10-6-10 (gem 10-6-10), and Amphiphilic Pyrimidinophane (APM).[23]

systems	$10^3 \times$ CMC (M)	$10^6 \times \Gamma_{max}$ (mol m^{-2})	A_{min} (nm^2)
B1[a]	1.7	0.71	2.34
DPC[b]	60.8	2.38	0.60
10-6-10[b,c]	7.0	0.76	2.20
APM[b,d]	1.0	1.45	1.14

[a] Water-DMF (20% vol). [b] Water. [c] See Figure 2S in the Supporting Information. [d] 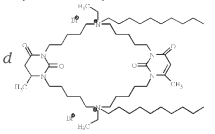

The cmc value of B1 extracted from these studies may be compared with that of a conventional single-head surfactant bearing the same alkyl radical, i.e. decylpyridinium chloride (DPC),[49] a gemini analogue 10-6-10 (gem 10-6-10) (see Figure 2S in the Supporting Information) and amphiphilic pyrimidinophane (APM) studied in work[23] (Table 1). As can be seen, cmc for **B1** is much lower as compared to DPC and even to gem 10-6-10. This effect cannot be attributed to the fact that mixed water-DMF solvent is used in the case of **B1**, because cmc usually increases in mixed water-organic media.[50−54] Cmc's of **B1** and APM are comparable. Probably these indicate that the association model of **B1** differs markedly from that of acyclic analogues. The surface excess Γ_{max} and the surface area per molecule, A_{min}, have been calculated using the Gibbs equation

$$\Gamma_{max} = \frac{1}{2.3nRT}\lim_{C \longrightarrow \text{cmc}}\left(\frac{d\pi}{d\log C}\right) \quad (1)$$

$$A_{min} = 1 \times 10^{18}/(N\Gamma_{max}) \quad (2)$$

were $R = 8.31$ J mol K^{-1} (gas constant), π is the surface pressure obtained from the surface tension of solvent minus the surface tension of the surfactant solution, and T is the absolute temperature in K, whereas $(d\pi/d\log C)$ is obtained from the tangency at the cmc. N_A is Avogadro's number (6.02×10^{23} mol^{-1}). The parameter n represents the number of species at the interface the concentration of which changes with surfactant concentration. The constant n takes the value 2 for an ionic surfactant where the surfactant ion and the counterion are univalent and the value 3 is taken for the dimeric surfactant made up of a divalent surfactant ion and two univalent counterions, in the absence of a swamping electrolyte.

One can find that the surface area per head group (A_{min}) for **B1** is higher than for other single head end even dimeric surfactants summarized in Table 1. This cannot be explained only by the bulky structure of **B1**, because macrocycle APM shows a

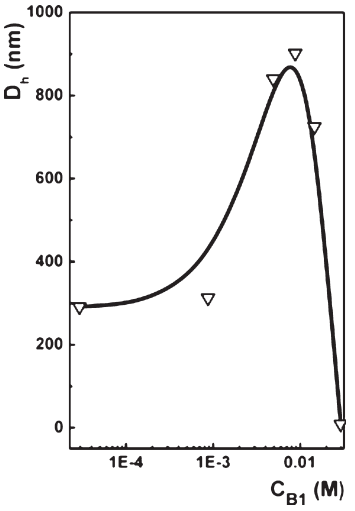

Figure 5. Effective hydrodynamic diameter versus concentration dependence for the water-DMF (20% vol) **B1** solution; 25 °C.

much lower parameter A_{min}. It should be assumed that a steric hindrance occurs around the head groups of **B1** originating from the specific packing mode, which prevents their approach. Additional shielding may be contributed by a high charge density at nitrogen resulting from their inaccessibility to counterions.

Examination of the Size of the B1 Aggregates by Methods of DLS and AFM. Figure 5 shows DLS data for the **B1** solutions obtained from the cumulant analysis of autocorrelation functions. As can be seen, an effective hydrodynamic diameter demonstrates a strong dependence on the **B1** concentration. A pronounced maximum is observed at the concentrations close to 0.009 M, whereupon a sharp decrease in the size occurs. Size distribution analysis presented in Figure 6 provides more detailed information on the aggregation behavior. Large aggregates are formed in the solutions beyond ca. 0.0009 M, i.e., in close proximity to cmc. At first, monomodal distribution is observed with D_h of 200 nm, while further, there appears the contribution of particles with ca. 800 nm.

An increase in the concentration results in an increase in the numbers of the dominant aggregates of 200 nm and the preservation of larger ones. Such behavior proceeds before the concentration of 0.009 M, which corresponds to the maximum in Figure 5. Further increase in the concentration is followed by a decrease in the effective diameter (Figure 5), which reflects the appearance of small aggregates with D_h of 8 nm. The solution becomes monodisperse at the highest concentration of 0.029 M, with only small aggregates existing. It should be mentioned that data in Figure 6 are obtained on the basis of spherical approximation and results in some simplification of the structural behavior of the systems. However, this approach makes it possible to obtain quantitative explanation of the concentration-dependent changes of properties of the systems.

With the results of the above studies summarized, one can conclude that sharp changes in the structure of aggregates are probably observed within the narrow concentration range of 0.009-0.01 M. This is supported by the following findings. (i) The second breakpoint occurs around 0.01 M in the surface tension isotherm and (less evidently) in the conductivity versus concentration plot. (ii) A maximum in the effective size of aggregates is observed within this range. (iii) The transition from large aggregates to small ones occurs. (iv) Gel-like behavior is observed with aging for the sample with the concentration of 0.009 M. Therefore, the

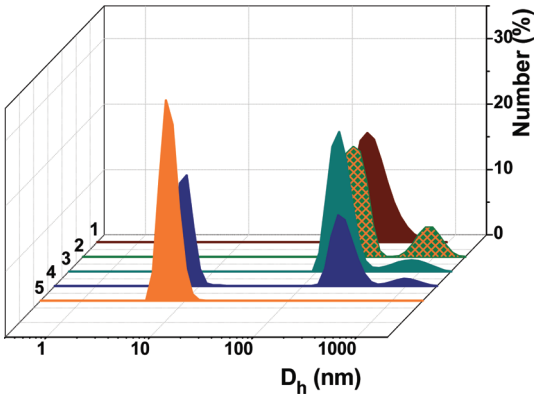

Figure 6. Size distribution for the water-DMF (20% vol) **B1** solution: 0.88 mM (1), 4.9 mM (2), 8.8 mM (3), 14.6 mM (4). 29.2 mM (5); 25 °C.

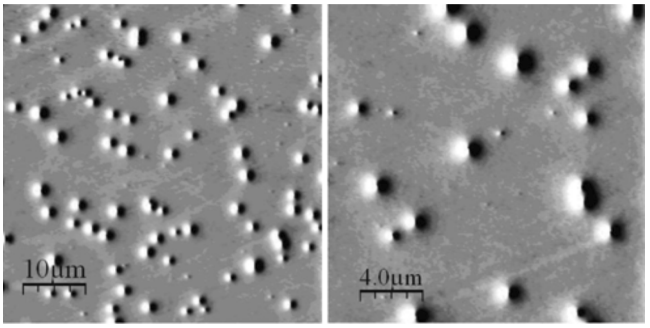

Figure 7. AFM images of the **B1** sample dried from its water-DMF (20% vol) solution: 0.009 M; 25°C.

assumption on two different models of association can be made, i.e. closed and open models. The former is typical for classical surfactants and results in the formation of small micelle-like aggregates, while the latter is characterized by the formation of the infinite structure (layer or stacks).[40] At low concentrations, **B1** is assumed to associate through the open model, while at higher concentration the closed model is involved.

Unfortunately, we fail to monitor in time the changes in the size of aggregates by the method of DLS because of the limitations of method, which originate from the low fluidity of samples. Therefore, an alternative technique is involved, i.e., AFM images are obtained (Figure 7), which reveal the mean particle size of 750 nm. As can be seen, the system is polydisperse, with two main contributions being observed, i.e., ca.700 nm (prevalent) and ca.250 nm (minor), although very large particles exceeding 1 micrometer are found as well. It can be assumed that an enlargement of aggregates occurs with aging. This idea is consistent with the data on zeta potential (Figure 8). The low value of +31 mV is observed for the samples at low concentrations (for comparison, the surface potential for CTAB exceeds +100 mV[55−57]) and diminishes practically to zero in the concentrated samples. Low ζ values and further neutralization of the charge probably favor the association of particles and the formation of gel-like systems. In addition, the formation of the hydrogen bond network is rather expected with the uracil and thiocytosin fragments involved. It was reported based on IR spectroscopy[58,59] and NMR spectroscopy[60] data that macrocycles consisting of two thiocytosine and one uracil moieties with the same structure as pyrimidinophane **1** form intra- and intermolecular hydrogen bonds in chloroform solutions via NH of thiocytosines as H-donors and C═O of

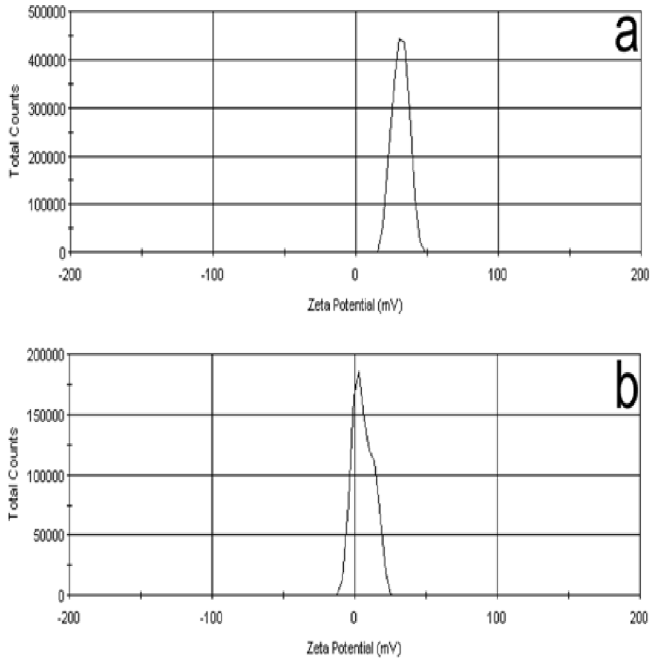

Figure 8. ζ values for the water-DMF (20% vol) **B1** solution at concentration of (a) 0.0009 and (b) 0.029 M; 25 °C.

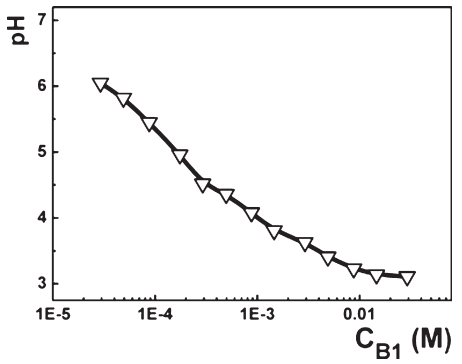

Figure 9. pH vs. **B1** concentration; water-DMF (20% vol); 25 °C.

uracil as H-acceptor. The same H-bonds can occur in solutions of the pyrimidinophanes with onium fragments in particular bola **B1**. It can be assumed that in the nonpolar interior of the **B1** aggregates, the combination of intra- and inter H-bonds dependent on the concentration of the pyrimidinophane is responsible for the observed effects. The gel formation probably reflects the instability of large particles, which provokes their further rearrangements. It is noteworthy that the charge neutralization is probably not underlain by the high affinity of aromatic tosylate anions to the micellar phase, as for typical surfactant systems. Tosylate anions are reported[24,25] to exert little effects on the aggregate size of acyclic and macrocyclic uracilic amphiphiles, and therefore the idea of viscoelastic behavior is not considered here. Meanwhile, uracilic amphiphiles with tosylate anions show quite specific solution behavior as compared to those with bromide counterions. As was earlier reported, an unusual decrease in solution pH with the concentration occurs.[24,25]

The same unusual results were obtained for the **B1** based system upon monitoring the solution pH (Figure 9). The following reasons may be assumed. Charged atoms of head groups are located in aromatic rings, which in turn are included in a macrocycle. This restricts the mobility of head groups and may result in their unfavorable orientation towards counterions. The competition between N^+ and NH atoms for their exposure to the aqueous phase may increase this effect. As a result, uncompensated charge would appear in the **B1** surface layer above the cmc and provoke a strong polarization up to the ionization of the water molecules in the solvate shells of head groups. Thus hydroxide ions and conjugated hydroxonium ions are generated. Unlike bulky organic ions, smaller hydroxide ions can bind with head groups, thereby compensating the charge, while residuary free protons acidify the system.

CONCLUSION

The new macrocyclic bolaamphiphile with uracil and thiocytosine fragments has been synthesized. Aggregation of **B1** has been studied by methods of tensiometry, conductometry, dynamic light scattering, and atomic force microscopy. Strong concentration-dependent structural behavior is revealed, which consists in the following. Monodisperse solution is observed at low surfactant concentration, with D_h of ca. 200 nm, whereas much smaller aggregates exist in concentrated systems with the single contribution of D_h = 8 nm. Intermediate concentration region is characterized by the contributions of both species. This structural transition is assumed to be underlain by two models of the association involved. These are open and closed models resulting in the formation of large "infinite" structures and small micelle-like aggregates respectively. Two breakpoints are revealed in the surface tension isotherms. The first one, around 0.002 M, is identified as a critical micelle concentration (cmc), whereas the second critical concentration of 0.01 M is a turning point between the two models. The growth of aggregates reaches a maximum at the concentration of 0.009 M, when the gel-like behavior appears. An unusual decrease in solution pH occurs with the concentration, initiated by the steric hindrance around the **B1** head groups.

Because of controllable structural behavior, **B1** can be offered as advanced building block for the design of soft matter, i.e., nanocontainer, nanoreactor, drug and gene carriers, etc. Indeed, because of the presence of onium fragments, uracil, and thiocytosine moieties, **B1** can bind with nucleic acid, which characterizes it as a candidate for development of nonviral vectors. This is our task in immediate future. One of the problem should be solved in this case is the compactization of DNA, i.e., the formation of amphiphile-DNA complex of the controllable dimension. Therefore the tool for control of the size behavior is strongly desirable in these biotechnologies. Furthermore, significant contribution in practice may be expected from phenomenon of a pH decrease in the B1 systems. As exemplified in Figure 3S (see the Supporting Information), such concentration-dependent pH behavior can be used for desirable regulation of the ratio of the acid and base forms of ionogenic compounds. This may elucidate one of mechanisms of high substrate specificity of enzyme catalysis. Therefore, the pH variable nanoreactors based on pyrimidinic surfactants analogous to those proposed in our work[25] are of importance from the viewpoint of development of biomimetic catalysts showing high substrate specificity towards the substrates of different hydrophobicity. Pyrimidinic macrocyclic amphiphiles especially B1 are documented to exhibit high antimicrobial activity.[61−63] This property together with surface activity and controllable gel behavior is important for preparation of cosmetics, antibacterial liniments, etc.

■ ASSOCIATED CONTENT

Supporting Information. Linear fitting of the conductivity data, tensiometry data of reference compound, UV−vis absorption spectrum (PDF). This material is available free of charge via the Internet at http://pubs.acs.org/.

■ AUTHOR INFORMATION

Corresponding Author

*E-mail: lucia@iopc.ru. Fax: +7 (843) 2732253. Tel: +7 (843) 273 22 93.

■ ACKNOWLEDGMENT

We thank the Russian Foundation for Basic Researches (Grants 10-03-00365), and the Russian Academy of Sciences (Chemistry and Material Science Division) for financial support and Valery M. Zakharov for his help with photo.

■ REFERENCES

(1) Yadava, P.; Buethe, D.; Hughes, J. In *Polymeric Drug Delivery I*; Svenson, S., Ed.; ACS Symposium Series; American Chemical Society: Washington, D.C., 2006; Vol. 923, pp 198−216.

(2) Vriezema, D.; Aragonès, M.; Elemans, J.; Cornelissen, J.; Rowan, A.; Nolte, R. *Chem. Rev.* **2005**, *105*, 1445–1490.

(3) Dwars, T.; Paetzold, E.; Oehme, G. *Angew. Chem., Int. Ed.* **2005**, *44*, 7174–7199.

(4) Tehrani-Bagha, A.; Holmberg, K. *Curr. Opin. Colloid Interface Sci.* **2007**, *12*, 81–91.

(5) Menger, F. M.; Keiper, J. S. *Angew. Chem., Int. Ed.* **2000**, *39*, 1906–1920.

(6) Xu, J.-P.; Ji, J.; Chen, W.-D.; Shen, J.-C. *Macromol. Biosci.* **2005**, *5*, 164–171.

(7) Alvarez, A. M.; Aida, J.; Francisco, M.; Luciano, G.; Viorel, P. N.; Alvaro, A.; Vazquez, T. J. *Langmuir* **2009**, *25*, 9037–9044.

(8) Suzuki, M.; Sato, T.; Shirai, H.; Hanabusa, K. *New J. Chem.* **2007**, *31*, 69–74.

(9) Jiang, L.; Wang, K.; Ke, F.; Liang, D.; Huang, J. *Soft Matter* **2009**, *5*, 599–606.

(10) Tsitsilianis, C. *Soft Matter* **2010**, *6*, 2372–2388.

(11) Steed, J. W.; Atwood, J. L. In *Supramolecular Chemistry*; Wiley: Chichester, U.K., 2000; p 745.

(12) Ghosh, A.; Dey, J. *Langmuir* **2009**, *25*, 8466–8472.

(13) Filippov, S. K.; Starovoytova, L.; Koňák, C.; Hruby, M.; Mackova, H.; Karlsson, G.; Stěpánek, P. *Langmuir* **2010**, *26*, 14450–14457.

(14) Shankar, B. V.; Patnaik, A. *J. Phys. Chem. B* **2007**, *111*, 9294–9300.

(15) Filippov, S.; Hruby, M.; Koňák, C.; Mackova, H.; Stěpánek, P. *Langmuir* **2008**, *24*, 9295–9301.

(16) Bao, H.; Li, L.; Leong, W. C.; Gan, L. H. *J. Phys. Chem. B* **2010**, *114*, 10666–10673.

(17) Wang, Y.; Zhang, J.; Zhang, W.; Zhang, M. *J. Org. Chem.* **2009**, *74*, 1923–1931.

(18) Sivakova, S.; Rowan, S. J. *Chem. Soc. Rev.* **2005**, *34*, 9–21.

(19) Song, B.; Wang, Z.; Chen, S.; Zhang, X.; Fu, Y.; Smet, M.; Dehaen, W. *Angew. Chem., Int. Ed.* **2005**, *44*, 4731–4735.

(20) Song, B.; Wei, H.; Wang, Z.; Zhang, X. *Adv. Mater.* **2007**, *19*, 416–420.

(21) Song, B; Wu, G.; Wang, Z.; Zhang, X.; Smet, M.; Dehaen, W. *Langmuir* **2009**, *25*, 13306–13310.

(22) Gissot, A.; Camplo, M.; Grinstaff, M. W.; Barthrelremy, P. *Org. Biomol. Chem.* **2008**, *6*, 1324–1333.

(23) Zakharova, L. Ya.; Semenov, V. E.; Voronin, M. A.; Valeeva, F. G.; Ibragimova, A. R.; Giniatullin, R. Kh.; Chernova, A. V.; Kharlamov, S. V.; Kudryavtseva, L. A.; Latypov, Sh. K.; Reznik, V. S.; Konovalov, A. I. *J. Phys. Chem. B.* **2007**, *111*, 14152–14162.

(24) Zakharova, L.; Syakaev, V.; Voronin, M.; Semenov, V.; Valeeva, F.; Ibragimova, A.; Bilalov, A.; Giniyatullin, R.; Latypov, Sh.; Reznik, V.; Konovalov, A. *J. Colloid Interface Sci.* **2010**, *342*, 119–127.

(25) Zakharova, L. Ya.; Semenov, V. E.; Voronin, M. A.; Valeeva, F. G.; Kudryavtseva, L. A.; Giniatullin, R. Kh.; Reznik, V. S.; Konovalov, A. I. *Mendel. Commun.* **2010**, *20*, 116–118.

(26) Nagarajan, R. *Chem. Eng. Commun.* **1987**, *55*, 251–273.

(27) Escamilla, G. H.; Newkome, G. R. *Angew. Chem., Int. Ed.* **1994**, *33*, 1937–1940.

(28) Fuhrhop, J.-H.; Köning, J. In *Molecular Assemblies and Membranes*; Stoddart, J. F., Eds.; Monographs in Supramolecular Chemistry; The Royal Society of Chemistry: London, 1994; Chapter I−XII, pp 1−227.

(29) Fuhrhop, J.-H.; Wang, T. *Chem. Rev.* **2004**, *104*, 2901–2938.

(30) Deinega, Y. F.; Ul'Berg, Z.; Marochko, L.; Rudi, V.; Denisenko, V. *Kolloid. Zh.* **1974**, *36*, 649–653.

(31) Menger, F. M.; Littau, C. A. *J. Am. Chem. Soc.* **1993**, *115*, 10083–10090.

(32) Rosen, M. J. *CHEMTECH* **1993**, *23*, 30–33.

(33) Zana, R.; Benrraou, M.; Rueff, R. *Langmuir* **1991**, *7*, 1072–1075.

(34) Menger, F. M.; Keiper, J. S. *Angew. Chem., Int. Ed.* **2000**, *39*, 1906–1920.

(35) Rosen, M. J.; Tracy, D. J. J. *J. Surfactants Deterg.* **1998**, *1*, 547–554.

(36) Zana, R. *Curr. Opin. Colloid Interface Sci.* **1996**, *1*, 566–571.

(37) Moreau, L.; Barthelemy, P.; Maataoui, M. E.; Grinstaff, M. W. *J. Am. Chem. Soc.* **2004**, *126*, 7533–7539.

(38) Iwaura, R.; Yoshida, K.; Masuda, M.; Yase, K.; Shimizu, T. *Chem. Mater.* **2002**, *14*, 3047–3053.

(39) Zakharova, L. Ya.; Kudryashova, Y. R.; Selivanova, N. M.; Voronin, M. A.; Ibragimova; A. R.; Solovieva, S. E.; Gubaidullin, A. T.; Litvinov, A. I.; Nizameev, I. R.; Kadirov, M. K.; Galyametdinov, Y. G.; Antipin, I. S.; Konovalov, A. I. *J. Membr. Sci.* **2010**, *364*, 90−101.

(40) Attwood, D. *Colloid Interface Sci.* **1995**, *55*, 271–303.

(41) Zakharova, L.; Mirgorodskaya, A.; Zhiltsova, E.; Kudryavtseva, L.; Konovalov, A. In *Reactions in Supramolecular Systems, Molecular Encapsulation: Organic Reactions in Constrained Systems*; Wiley: New York, 2010; pp 397−420.

(42) Zakharova, L.; Mirgorodskaya, A.; Zhiltsova, E.; Kudryavtseva, L.; Konovalov, A. *Russ. Chem. Bull., Int. Ed.* **2004**, *53*, 1385–1401.

(43) Mikhailov, A. S.; Skuzlova, V. I.; Pashkurov, N. G.; Reznik, V. S. *Russ. J. Gen. Chem.* **1997**, *66*, 500–503.

(44) Semenov, V. E.; Voloshina, A. D.; Kulik, N. V.; Uraleva, S. Y.; Zobov, V. V.; Giniyatullin, R. Kh.; Mikhailov, A. S.; Akamsin, V. D.; Efremov, Y. Y.; Reznik, V. S. *Pharm. Chem. J.* **2009**, *43*, 448–453.

(45) Zakharova, L.; Ibragimova, A.; Valeeva, F.; Zakharov, A.; Mustafina, A.; Kudryavtseva, L.; Harlampidi, H.; Konovalov, A. *Langmuir* **2007**, *23*, 3214–3224.

(46) Zakharova, L.; Valeeva, F.; Zakharov, A.; Ibragimova, A.; Kudryavtseva, L.; Harlampidi, H. *J. Colloid Interface Sci.* **2003**, *263*, 597–605.

(47) Kozlov, A.; Semenov, V.; Mikhailov, A.; Aganov, A.; Smith, M.; Reznik, V.; Latypov, Sh. *J. Phys. Chem. B* **2008**, *112*, 3259–3267.

(48) Mikhailov, A. S.; Giniyatullin, R. Kh.; Semenov, V. E.; Reznik, V. S.; Nafikova, A. A.; Latypov, S. K.; Efremov, Y. Y.; Sharafutdinova, D. R. *Russ. Chem. Bull., Int. Ed.* **2003**, *52*, 1399–1402.

(49) Zakharov, A. V.; Voronin, M. A.; Valeeva, F. G.; Gubanov, E. F. Proceedings of the Conference "Structure and Dynamics of Molecular Systems"; Kazan, 2003, Vol. *10*, Pt. 2, pp 89−92.

(50) Graciani, M. M.; Muñoz, M.; Rodríguez, A.; Moyá, M. L. *Langmuir* **2005**, *21*, 3303–3310.

(51) Nagarajan, R.; Wang, C.-C. *Langmuir* **2000**, *16*, 5242–5251.

(52) Sarkar, B.; Lam, S.; Alexandridis, P. *Langmuir* **2010**, *26*, 10532–10540.

(53) Kabir-ud-Din; Koya, P. A. *Langmuir* **2010**, *26*, 7905–7914.

(54) Kabir-ud-Din; Koya, P. A. *J. Chem. Eng. Data* **2010**, *55*, 1921–1929.
(55) Zakharova, L. Ya.; Fedorov, S. B.; Kudryavtseva, L. A.; Bel'skiy, V. E.; Ivanov, B. E. *Izv. AN SSSR, Ser. Chim.* **1990**, *5*, 991–994.
(56) Taranskar, P.; Jana, N. R. *Langmuir* **1996**, *12*, 3114–3121.
(57) Adamczyk, Z.; Para, G.; Warszynski, P. *Langmuir* **1999**, *15*, 8383–8387.
(58) Shagidullin, R. R.; Chernova, A. V.; Doroshkina, G. M.; Kataev, V. E.; Bazhanova, Z. G.; Katsyuba, S. A.; Reznik, V. S.; Mikhailov, A. S.; Giniyatullin, R. Kh.; Pashkurov, N. G.; Efremov, Yu. Ya.; Nafikova, A. A. *Russ. J. Gen. Chem.* **2002**, *72*, 1625–1632.
(59) Shagidullin, R. R.; Chernova, A. V.; Bazhanova, Z. G.; Lii, J.-H.; Kataev, V. E.; Katsyuba, S. A.; Reznik, V. S. *J. Mol. Struct.* **2004**, *707*, 1–9.
(60) Kozlov, A. V.; Semenov, V. E.; Mikhailov, A. S.; Reznik, V. S.; Latypov, S. K. *Tetrahedron Lett.* **2008**, *49*, 6674–6678.
(61) Semenov, V. E.; Voloshina, A. D.; Toroptzova, E. M.; Kulik, N. V.; Zobov, V. V.; Giniyatullin, R. Kh.; Mikhailov, A. S.; Nikolaev, A. E.; Akamsin, V. D.; Reznik, V. S. *Eur. J. Med. Chem.* **2006**, *41*, 1093–1101.
(62) Semenov, V. E.; Voloshina, A. D.; Kulik, N. V.; Uraleva, S. Y.; Zobov, V. V.; Giniyatullin, R. Kh.; Mikhailov, A. S.; Akamsin, V. D.; Efremov, Y. Y.; Reznik, V. S. *Pharm. Chem. J.* **2009**, *43*, 448–453.
(63) Nikolaev, A.E.; Semenov, V. E.; Voloshina, A. D.; Kulik, N. V.; Reznik, V. S. *Pharm. Chem. J.* **2010**, *44*, 130–133.